Phase separation in the presence of spatially periodic forcing

A. P. Krekhov and L. Kramer
Physikalisches Institut, Universität Bayreuth, D-95440 Bayreuth, Germany
(Received 4 June 2004; published 3 December 2004)

We have investigated theoretically phase separation in the presence of spatially periodic forcing. From the analytic and numeric study of a suitably generalized Cahn-Hilliard equation in one and two dimensions, we find that the forcing amplitude necessary to generate a periodic kink-type state from small random initial conditions depends weakly on wave number. This amplitude is much larger than the one necessary to stabilize the periodic state, i.e., to prevent late-stage coarsening, once it is established. Surprisingly, the destabilizing mode is of long-wave type, which is in contrast to the well-known most rapidly growing coarsening mode in the unforced system. In the Allen-Cahn equation with nonconserved order parameter the relevant modes are always long wave. It appears feasible to observe these effects by imposing a temperature modulation by optical grating which then couples to concentration modulation via the (Ludwig-)Soret effect.

DOI: 10.1103/PhysRevE.70.061801 PACS number(s): 61.41.+e, 64.75.+g, 47.54.+r

I. INTRODUCTION

The process of phase separation in a quenched system has been the subject of many theoretical and experimental investigations in the field of small molecular or atomic systems, such as binary alloys, fluid mixtures, and inorganic glasses [1,2]. When such a system at the critical composition is quenched from a homogeneous, usually high-temperature phase to a point sufficiently below the coexistence curve (a critical quench), a small-amplitude, long-wavelength instability develops. This phenomenon is known as spinodal decomposition (SD). The term originally refers to the initial stage of phase separation which occurs in a quenched, thermodynamically unstable, solid solution. Among the various kinetic mechanisms associated with first-order phase transitions, SD is distinguished from, say, nucleation and growth in that it requires no thermal activation energy; that is, it occurs in the unstable rather than in the metastable region of a phase diagram. A second distinguishing characteristic is that the order parameter which describes the system, usually the composition variable (concentration), obeys a local conservation law. Thus the decomposition is limited by diffusionlike processes and, in its later stages, exhibits very slow coarsening rather than the more rapid approach to completion which occurs in magnetic or structural phase transitions without conserved order parameter ($l \sim t^{1/2}$). At later times, the small inhomogeneities in the order parameter evolve into macroscopic domains of one or the other phase and an interconnected structure is formed.

The study of phase separation in polymer blends has been of considerable technological importance in order to develop new materials to achieve specific properties. The high molecular weight and chainlike nature of polymers results in a small entropy of mixing, and thus in a large region of immiscibility (comparatively high critical temperatures). It is well known that the morphological and interfacial properties of these systems play an important role in most of their practical applications.

In recent years, the dynamics of SD in polymer blends has attracted much experimental and theoretical interest, due to the fact that (i) it became quite clear that polymeric mixtures belong to the same universality class as binary alloys and low molecular weight fluid mixtures and (ii) in these materials it is relatively easy to probe different regions of the phase diagram over widely varying time scales.

When phase separation occurs by SD, a polymer blend destabilizes with respect to long wavelength concentration fluctuations. Although mixtures become increasingly susceptible to external perturbations as the critical point is approached, the response changes qualitatively when the mixture is quenched into the two-phase region. The system is then in an unstable state away from equilibrium and perturbations can be amplified and have a large scale influence on the phase separation process. The beneficial aspect of this sensitivity of phase separation and other pattern formation processes to perturbations is that it offers substantial opportunities to control the morphology of the evolving patterns.

Up to now a large number of studies on phase separation in polymer mixtures have considered the application of external fields (flow [3], gravitational field [4], concentration [5], and temperature [6] gradients, chemical reactions, and cross linking [7], etc.) with an attempt to elucidate the time evolution of the structures. However, this did not lead to substantial control over the morphology.

Motivated by experiments [8,9] we here focus on phase separation in the presence of spatially periodic driving arising from thermal diffusion (Ludwig-Soret effect [10]) caused by an inhomogeneous temperature distribution in the polymer film. Starting with the standard Cahn-Hilliard (CH) theory [11] we have developed the description of SD taking into account spatially periodic temperature modulation that could be created in optical grating experiments as in Refs. [8,9].

The paper is organized as follows. In Sec. II we introduce the modified CH equations and define the relation between model parameters and those of polymer blend theory. In Sec. III the results of one-dimensional (1D) analysis of the stability of periodic structures are presented and compared with systematic simulations. Section IV is devoted to the results of representative 2D simulations. Finally, in Sec. V the results are discussed and put into perspective.

II. THEORETICAL BACKGROUND

The main ingredient of the CH theory of phase separation [11] is a conserved field variable representing the local concentration of one of the components of the binary mixture (or, sometimes, the difference between the local concentration of the two components). Let $\phi(\mathbf{r},t)$ denote the local volume fraction of component A. Then for an incompressible binary A/B mixture the local concentration of the B component is $[1-\phi(\mathbf{r},t)]$. The continuity equation relates the spatial and time dependence of the concentration $\phi(\mathbf{r},t)$ to the mass current $\mathbf{j}(\mathbf{r},t)$, and expresses the conservation of mass in the system,

$$\frac{\partial\phi(\mathbf{r},t)}{\partial t} = -\boldsymbol{\nabla}\cdot\mathbf{j}(\mathbf{r},t). \tag{1}$$

The mass current can be related to gradients of the chemical potential $\mu(=\mu_A-\mu_B)$ and of the temperature T, and the mass current $\mathbf{j}_T(\mathbf{r},t)$ arising from thermal fluctuations,

$$\mathbf{j}(\mathbf{r},t) = -M\boldsymbol{\nabla}\mu - D_T\phi(1-\phi)\boldsymbol{\nabla}T(\mathbf{r},t) + \mathbf{j}_T(\mathbf{r},t), \tag{2}$$

where M is the "mobility" of species A with respect to B (often treated as a constant although in general it would depend on concentration). In a Ginzburg-Landau-type continuum description the chemical potential μ is related thermodynamically to the free energy functional $F[\phi(\mathbf{r},t)]$,

$$\mu = \frac{\delta F[\phi]}{\delta\phi},\ \frac{F[\phi]}{k_BT} = \frac{1}{v}\int d\mathbf{r}\left[\frac{f[\phi]}{k_BT} + \kappa(\phi)(\nabla\phi)^2\right], \tag{3}$$

where k_B is Boltzmann's constant. We start from a lattice model and then v is the volume per lattice site, and $f[\phi]$ is the local, homogeneous, coarse-grained free energy density of mixing which has a double-well structure in the two-phase region. The square gradient term expresses the unfavorable nature of interfaces. It describes the energy necessary to create an interface between homogeneous A-rich and B-rich domains. We take the Flory-Huggins (FH) expression for the free energy of mixing (per lattice site) for an incompressible binary polymer blend,

$$\frac{f}{k_BT} = \frac{\phi}{N_A}\ln\phi + \frac{(1-\phi)}{N_B}\ln(1-\phi) + \chi\phi(1-\phi), \tag{4}$$

where N_A, N_B are the "chain lengths" (degrees of polymerization) of species A and B, respectively; χ is the Flory interaction parameter that measures the strength of interaction between species A and B and favors phase separation when it is positive. The value of χ depends on the temperature and is usually taken as

$$\chi = \alpha + \beta T^{-1}, \tag{5}$$

where α and β are empirical constants [12]. For the coefficient of the gradient term we use de Gennes' random phase approximation,

$$\kappa(\phi) = \frac{1}{36}\left[\frac{\sigma_A^2}{\phi} + \frac{\sigma_B^2}{1-\phi}\right], \tag{6}$$

where σ_A and σ_B are the monomer sizes (Kuhn lengths) of the A and B components, respectively.

Since we have in mind polymer blends subjected to an inhomogeneous temperature field produced by light absorption, the heat equation should be added to the model,

$$\frac{\partial T(\mathbf{r},t)}{\partial t} = D_{th}\nabla^2T(\mathbf{r},t) + \frac{\alpha_\lambda}{\rho c_p}I(\mathbf{r},t). \tag{7}$$

The heat source term is proportional to the light intensity I that corresponds to the experimental situation where the spatially periodic temperature modulation is created by means of the interference grating of intersecting laser beams or local illumination of the polymer film [8]. Here α_λ is the optical absorption coefficient, ρ is the density, and c_p the specific heat at constant pressure. For the typical polymer blends under experimental study the ratio of the temperature diffusion time over the mass diffusion time is of the order of 10^{-3} therefore one can treat the heat equation (7) in the steady limit (neglect the time derivative of the temperature).

The mixture of composition ϕ_0 is unstable against phase separation when $f[\phi]$ has negative curvature at $\phi=\phi_0$. One easily finds that the critical point of SD in model (4) is given by

$$\phi_c = N_B^{1/2}/(N_A^{1/2}+N_B^{1/2}),$$

$$\chi_c = [N_A^{1/2}+N_B^{1/2}]^2/(2N_AN_B), \tag{8}$$

such that the system is miscible for $\chi<\chi_c$ and immiscible for $\chi>\chi_c$ at the critical concentration. Close to (ϕ_c,χ_c) the FH expression for the free energy can be approximated by a Taylor expansion with respect to the composition fluctuation $\varphi(\mathbf{r},t)=[\phi(\mathbf{r},t)-\phi_c]$ leading to the Ginzburg-Landau functional (an irrelevant term linear in φ has been omitted)

$$\frac{F_{GL}[\varphi]}{k_BT_c} = \frac{1}{v}\int d\mathbf{r}\left[\frac{1}{2}b\varphi^2 + \frac{1}{4}u\varphi^4 + \frac{1}{2}K(\nabla\varphi)^2\right], \tag{9}$$

where the coefficients are defined as

$$b = 2(\chi_c-\chi) \approx \frac{2\beta}{T_c^2}(T-T_c),\ u = \frac{4}{3}\chi_c^2\sqrt{N_AN_B},$$

$$K = \frac{1}{18}[\sigma_A^2(1+\sqrt{N_A/N_B}) + \sigma_B^2(1+\sqrt{N_B/N_A})]. \tag{10}$$

Equations (1) and (7) in combination with Eqs. (2) and (9) define our model close to the critical point,

$$\frac{\partial\varphi(\mathbf{r},t)}{\partial t} = \frac{Mk_BT_c}{v}\nabla^2[b\varphi + u\varphi^3 - K\nabla^2\varphi] + D_T\phi_c(1-\phi_c)\nabla^2T + \eta(\mathbf{r},t), \tag{11}$$

$$D_{th}\nabla^2T = -\frac{\alpha_\lambda}{\rho c_p}I(\mathbf{r},t). \tag{12}$$

Note that the quantity $S_T=D_T/D$ is the Soret coefficient with the diffusion coefficient

$$D = (Mk_BT_c|b|)/v. \tag{13}$$

In the case of optical grating experiments $I(\mathbf{r},t)=I_0\cos(qx)$ [8]. Then

$$\nabla^2 T = -\delta T_0 q^2 \cos(qx), \quad \delta T_0 = \frac{\alpha_\lambda}{\rho c_p D_{th}} \frac{I_0}{q^2}. \tag{14}$$

The thermal noise term $\eta(\mathbf{r},t)$ is Gaussian, δ correlated, and satisfies the fluctuation-dissipation theorem, which gives

$$\eta(\mathbf{r},t) = \sqrt{2Mk_B T_c}\zeta(\mathbf{r},t),$$

$$\langle \zeta(\mathbf{r},t) \rangle = 0,$$

$$\langle \zeta(\mathbf{r},t)\zeta(\mathbf{r}',t') \rangle = -\nabla^2 \delta(\mathbf{r}-\mathbf{r}')\delta(t-t'). \tag{15}$$

In the absence of thermal diffusion Eq. (11) reduces to the well known CH equation (model *B* [13]). In fact, Eq. (11) gives a universal description of a system in the vicinity of a critical point leading to SD. The derivation from the Flory-Huggins model was presented in order to estimate roughly the parameters for polymer blends (see Sec. V).

We introduce dimensionless variables by choosing the temperature T_0 after the quench as our reference temperature ($T_0 < T_c$) and write

$$\mathbf{r} = \mathbf{r}'\xi, \ \xi = (K/|b|)^{1/2};$$

$$t = t'\tau, \ \tau = \xi^2/D;$$

$$\varphi = \psi(u/|b|)^{-1/2}, \tag{16}$$

where all quantities are evaluated at T_0. We then obtain (primes are omitted)

$$\frac{\partial \psi(\mathbf{r},t)}{\partial t} = \nabla^2[-\epsilon\psi + \psi^3 - \nabla^2\psi + a\cos(qx)] + \sqrt{g}\zeta(\mathbf{r},t), \tag{17}$$

where

$$\epsilon = \frac{T_c - T}{T_c - T_0}, \ a = \frac{D_T}{D}\left(\frac{u}{|b|}\right)^{1/2} \phi_c(1-\phi_c)\delta T_0,$$

$$g = 2vu\xi^{-d/2}b^{-2}. \tag{18}$$

Equation (17) describes the dynamics of phase separation following a quench from the stable one-phase region ($\epsilon < 0$) to the reference temperature in the two-phase region ($\epsilon = 1$). In the following we will consider only the case of a symmetric quench where initially, at $t=0$, one has $\int d\mathbf{r}\psi = 0$.

In the absence of the forcing ($a=0$), in the linear regime, one has exponential growth of modes with wave number q with rate $\sigma = q^2(1-q^2)$. Thus growth is limited to $q^2 < 1$ and the fastest growth is for $q^2 = 1/2$. A system can be treated as quasi-1D or quasi-2D if the transverse dimensions are small compared to the growing modes.

As is seen from Eq. (17), the dimensionless noise strength g is a measure of the quench depth. The parameter g can be related to the Ginzburg criterion for the validity of mean-field theory as formulated by Binder for SD [14]. In the absence of the forcing the Ginzburg criterion gives (see Appendix)

$$g \ll 4V(K/|b|)^{-d/2}, \tag{19}$$

where $V \sim r_m^d$ is a coarse-graining volume. For T close to T_c the only relevant length scale is the correlation length ξ. Therefore the extreme (from below) possible choice for r_m would be $r_m = \alpha(K/|b|)^{1/2}$ where $\alpha \geqslant 1$ and Eq. (19) reduces to

$$g \ll 4\alpha^d. \tag{20}$$

For $d \leqslant 3$ this restricts T_0 to temperatures not too near to T_c [see Eqs. (18) and (10)]. In the following we will consider essentially only the mean-field regime where one can omit the noise term in Eq. (17).

In the case of a nonconserved order parameter the CH equation (17) is replaced by the usual real Ginzburg-Landau equation, which in the context of phase separation is known as the Allen-Cahn equation. It is obtained by replacing in Eq. (17) the operator ∇^2 acting on the square bracket by -1.

III. 1D SIMULATIONS AND ANALYSIS

A. Numerical simulations

We have studied the dynamics described by Eq. (17) in the 1D case where $\psi = \psi(x,t)$. Since weak thermal noise only affects the initial stages of the phase separation [15] we discard permanent noise in what follows. In the one-phase region ($\epsilon < 0$) one has stable, stationary solutions of Eq. (17) that exhibit a small-amplitude spatial oscillation (for small driving amplitude a) with period $2\pi/q$, i.e., the driving stimulates a concentration modulation with the amplitude proportional to the driving amplitude a. When the system is quenched into the two-phase region ($\epsilon > 0$; one may choose $\epsilon = 1$) the SD sets in and the late stage of the process depends on the amplitude of periodic driving. For numerical simulations of the noiseless Eq. (17) a central finite difference approximation of the spatial derivative with fourth order Runge-Kutta integration of the resulting ordinary differential equations in time have been used. The typical system size was $L = 512$ and some test runs were made with $L = 1024$ and 2048. We used a mesh size $\delta x = 0.5$ and time step $\delta t = 1 \times 10^{-2}$. The accuracy of calculations was checked by choosing $\delta x = 0.25$ and $\delta t = 5 \times 10^{-4}$. For initial condition we took small fluctuations around the homogeneous (single phase) state $\psi = 0$ by assigning to each lattice site a random number uniformly distributed in the interval ± 0.01. In order to average over initial random configurations 100 runs were performed. Our numerical simulations show that there is a well-defined critical amplitude $a_c = a_c(q)$, above which the time evolution of the system always ends up in the stationary, kink-type periodic solution (for not too large q) with the period $2\pi/q$, independent of the initial conditions. In contrast to the situation for $\epsilon < 0$, the solution is in antiphase with the driving, i.e., ψ is positive where the driving is negative. In Fig. 1 the critical amplitude $a_c(q)$ is shown (solid line) as obtained efficiently from the numerical simulations ($\epsilon = 1$).

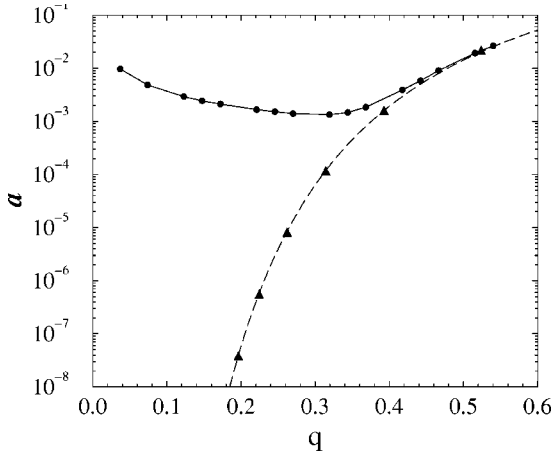

FIG. 1. The critical driving amplitude a_c above which the evolution of the system ends up in a stationary, kink-type periodic solution (solid line). Linear stability analysis of the periodic solution: numerical (triangles) and approximate analytical results for a_s from Eq. (42) (dashed line).

B. Stability analysis

In an attempt to gain an understanding of the magnitude of $a_c(q)$ we have performed a linear stability analysis of the periodic solution $\psi_s(x)$ of the noiseless Eq. (17) ($\epsilon=1$). Thus we write

$$\psi(x,t) = \psi_s(x) + e^{\sigma t}\phi(x), \tag{21}$$

where

$$-\psi_s + \psi_s^3 - \partial_{xx}\psi_s + a\cos(qx) = 0 \tag{22}$$

with periodic boundary conditions $\psi_s(0)=\psi_s(L)$ and L is the system length. Substituting Eq. (21) into Eq. (17) and linearizing in the perturbation ϕ one gets for the growth rate

$$\sigma\phi = \partial_{xx}\mathcal{L}\phi,\ \mathcal{L} = -1 + 3\psi_s^2 - \partial_{xx}. \tag{23}$$

One expects that ϕ can be represented in Floquet form,

$$\phi(x) = e^{ipx}\phi_F(x), \tag{24}$$

where $\phi_F(x)$ is $2\pi/q$ periodic. Since the critical driving amplitude a which stabilizes ψ_s is very small (see Fig. 1) we look for the solution of Eqs. (22) and (23) in a perturbative way,

$$\psi_s = \psi_{s0} + a\psi_{s1} + \cdots,$$

$$\phi = \phi_0 + a\phi_1 + \cdots,$$

$$\sigma = \sigma_0 + a\sigma_1 + \cdots \tag{25}$$

and

$$\mathcal{L} = \mathcal{L}_0 + a\mathcal{L}_1 + \cdots,$$

$$\mathcal{L}_0 = -1 + 3\psi_{s0}^2 - \partial_{xx},$$

$$\mathcal{L}_1 = 6\psi_{s0}\psi_{s1}, \tag{26}$$

where from Eq. (22)

$$-\psi_{s0} + \psi_{s0}^3 - \partial_{xx}\psi_{s0} = 0, \tag{27}$$

$$\mathcal{L}_0\psi_{s1} = -\cos(qx). \tag{28}$$

Substituting the expansion (25) into Eq. (23) and collecting the terms at zero and first order, we obtain

$$\sigma_0\phi_0 - \partial_{xx}\mathcal{L}_0\phi_0 = 0, \tag{29}$$

$$\sigma_0\phi_1 - \partial_{xx}\mathcal{L}_0\phi_1 = -\sigma_1\phi_0 + \partial_{xx}\mathcal{L}_1\phi_0. \tag{30}$$

Following the approach developed for the stability analysis of the standard CH equation ($a=0$) [16] we define a "conjugate" $\tilde{\phi}_0$ by

$$\partial_{xx}\tilde{\phi}_0 = \phi_0, \tag{31}$$

where $\tilde{\phi}_0$ also satisfies periodic boundary conditions. Projecting Eqs. (29) and (30) onto $\tilde{\phi}_0$ one obtains

$$\sigma_0\langle\tilde{\phi}_0,\phi_0\rangle = \langle\phi_0,\mathcal{L}_0\phi_0\rangle \tag{32}$$

and the solvability condition for ϕ_1,

$$\sigma_1\langle\tilde{\phi}_0,\phi_0\rangle = \langle\phi_0,\mathcal{L}_1\phi_0\rangle. \tag{33}$$

Thus, at first order in a, the critical amplitude a_s for $\sigma\approx\sigma_0 + a\sigma_1 = 0$ is

$$a_s = -\frac{\langle\phi_0,\mathcal{L}_0\phi_0\rangle}{\langle\phi_0,\mathcal{L}_1\phi_0\rangle}. \tag{34}$$

We will use the "tight-binding approximation" [16] where only nearest-neighbor overlap integrals are kept in the calculation of the projection integrals in Eqs. (32)–(34). Without driving ($a=0$) the stationary periodic solution ψ_{s0} can be approximated as a periodic array of M single interfaces with spacing π/q ($L=\pi M/q$),

$$\psi_{s0} \approx \sum_{n=1}^{M}(-1)^{n-1}\tanh\left(\frac{1}{\sqrt{2}}[x-(n-1/2)\pi/q]\right) - 1. \tag{35}$$

This leads to [see Eq. (26)]

$$\mathcal{L}_0 \approx 2 - 3\sum_{n=1}^{M}\operatorname{sech}^2\left(\frac{1}{\sqrt{2}}[x-(n-1/2)\pi/q]\right) - \partial_{xx}. \tag{36}$$

A good trial function ϕ_0 is obtained by superposing small translations of the kinks,

$$\phi_0 \approx \frac{1}{\sqrt{M}}\sum_{n=1}^{M} e^{i(n-1)p\pi/q}\operatorname{sech}^2\left(\frac{x-(n-1/2)\pi/q}{\sqrt{2}}\right), \tag{37}$$

where $p/q=2m/M$ (m is integer), or equivalently, $p=2\pi m/L$. Note that $m=0$ is not allowed since it violates the conservation law. Keeping only nearest-neighbor overlap integrals in Eq. (32) we recover the result of Langer [16] for the growth rate σ_0

$$\langle \tilde{\phi}_0, \phi_0 \rangle = -\frac{4\pi/q}{1-\cos(p\pi/q)},$$

$$\langle \phi_0, \mathcal{L}_0 \phi_0 \rangle = -[1+\cos(p\pi/q)]64\sqrt{2}e^{-\sqrt{2}\pi/q}, \quad (38)$$

and

$$\sigma_0(q,p) = \frac{\langle \phi_0, \mathcal{L}_0 \phi_0 \rangle}{\langle \tilde{\phi}_0, \phi_0 \rangle} = \sin^2(p\pi/q)16\sqrt{2}\frac{e^{-\sqrt{2}\pi/q}}{(\pi/q)}. \quad (39)$$

This demonstrates that for the unforced system the most unstable mode has Floquet exponent $p=\pm q/2$ corresponding to a period-doubling process.

Using Eq. (36) one finds the approximate solution of Eq. (28) for $q \ll 1$,

$$\psi_{s1} \approx -\frac{1}{2}\cos(qx). \quad (40)$$

Keeping again only nearest-neighbor overlap integrals in $\langle \phi_0, \mathcal{L}_1 \phi_0 \rangle$ and expanding Eq. (40) around its zeros one finally finds from Eq. (34)

$$\langle \phi_0, \mathcal{L}_1 \phi_0 \rangle = 4q\left(1-\frac{\pi^2 q^2}{12}\right) \quad (41)$$

and

$$a_s(q,p) = [1+\cos(p\pi/q)]\frac{16\sqrt{2}}{q}e^{-\sqrt{2}\pi/q}\left(1+\frac{\pi^2 q^2}{12}\right). \quad (42)$$

This result shows that the onset of instability in the forced system (largest a_s) occurs for Floquet exponent $p \to 0$, i.e., surprisingly, corresponds to long-wave modulation (we remind that $p \neq 0$).

Let us contrast this with the nonconserved case described by the Allen-Cahn equation. There the expression for the critical amplitude a_s is unchanged, i.e., Eqs. (34) and (42) remain valid. On the other hand, the growth rate σ_0 for the unforced system is

$$\sigma_0 = -\frac{\langle \phi_0, \mathcal{L}_0 \phi_0 \rangle}{\langle \phi_0, \phi_0 \rangle} = [1+\cos(p\pi/q)]48e^{-\sqrt{2}\pi/q}. \quad (43)$$

Thus in the Allen-Cahn equation the p dependence of a_s and σ_0 are the same. Therefore, in contrast to the CH equation, the most unstable mode for the Allen-Cahn equation always has Floquet exponent $p=0$.

In Fig. 2 the growth rates $\sigma(a)=\sigma_0+a\sigma_1$ as a function of the driving amplitude a are presented for the CH equation and for comparison also for the Allen-Cahn equation. In order to test these results we have also performed a numerical linear stability analysis of the periodic solutions. The system size was $L=256$ and $q=\pi/16$ with periodic boundary conditions. The numerical results are indistinguishable from our analytic results for $\sigma(a)=\sigma_0+a\sigma_1$ and this remains the case for $q<\pi/8$.

The relevant critical amplitude for the stabilization of the periodic pattern is given by $a_s(q,p)$ taken in the limit $p \to 0$. In Fig. 1 this quantity, as given from Eq. (42), is included (dashed line). Also given are the corresponding numerical results (triangles). The small differences arising for $q \geqslant 0.4$ cannot be resolved on the logarithmic scale of the figure. As expected, the corresponding critical eigenfunction exhibits a long-wave modulated superposition of kink translations.

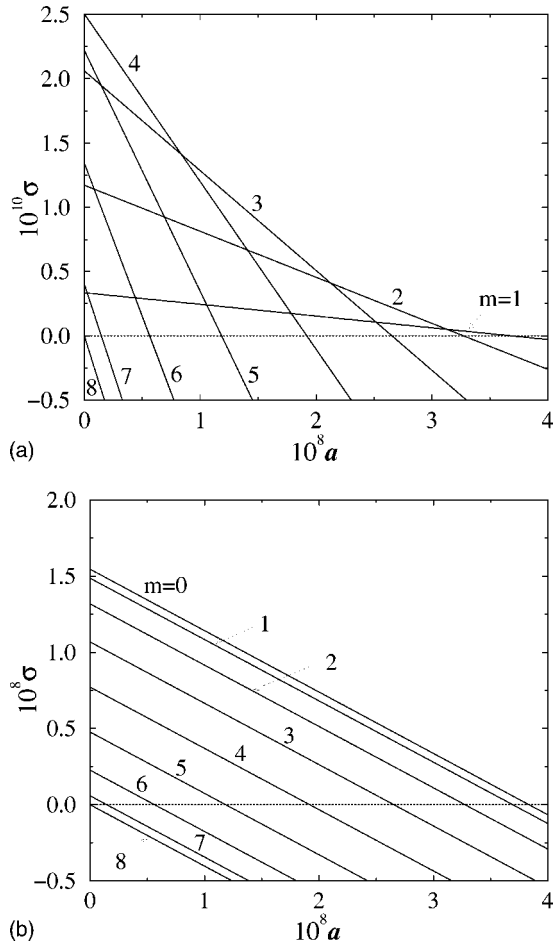

FIG. 2. The growth rates $\sigma(a)=\sigma_0+a\sigma_1$ for the Cahn-Hilliard (a) and the Allen-Cahn (b) equation as a function of driving amplitude a calculated analytically for $q=\pi/16$ and various values of $p/q=m/8$. $m=4$ corresponds to the period-doubling case.

Since linear stability of the periodic solution is a necessary condition for it being an attractor one has $a_c(q) \geqslant a_s(q)$. For q approaching the fastest growing wave number $q=1/\sqrt{2}$ one has $a_c(q) \approx a_s(q)$ (see Fig. 1), which is actually not surprising, and this value gives a reasonable estimate for $a_c(q)$ also for smaller values of q.

IV. 2D SIMULATIONS

We have performed extended simulations of the noiseless Eq. (17) in two dimensions. The phase separation process after the quench can be characterized by the structure factor

$$S(\mathbf{k},t) = |\hat{\psi}(\mathbf{k},t)|^2, \ \hat{\psi}(\mathbf{k},t) = \int d\mathbf{r} e^{i\mathbf{k}\cdot\mathbf{r}}\psi(\mathbf{r},t), \quad (44)$$

which can be measured experimentally and allows direct comparison with the predictions. For the standard CH equa-

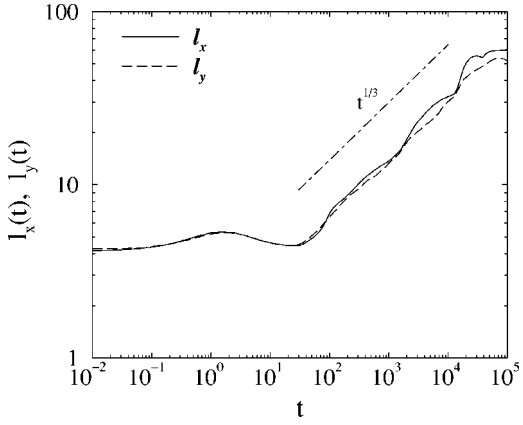

FIG. 3. Dynamics of the characteristic length scales $l_x(t)$ and $l_y(t)$ without driving ($a=0$). System size $L_x=L_y=256$, $\epsilon=1$.

tion the structure factor is isotropic $S=S(|\mathbf{k}|,t)$ and possesses at long times the universal scaling behavior $S(k,t) \sim l(t)^d G[kl(t)]$ where the characteristic length of domains $l(t)\sim t^{1/3}$ (for $d\geqslant 2$) [1]. With the spatially periodic driving we may expect an anisotropy of the structure factor. The average domain length in the x and y directions can be related to the characteristic length scales,

$$l_x(t)=[\langle k_x\rangle(t)]^{-1},\ l_y(t)=[\langle k_y\rangle(t)]^{-1}, \tag{45}$$

where

$$\langle k_x\rangle(t)=\frac{\int dk_x S(k_x,0,t)k_x}{\int dk_x S(k_x,0,t)},$$

$$\langle k_y\rangle(t)=\frac{\int dk_y S(0,k_y,t)k_y}{\int dk_y S(0,k_y,t)}. \tag{46}$$

Numerical simulations of Eq. (17) were performed using again central finite difference approximation of the spatial derivatives with fourth order Runge-Kutta integration of the resulting ordinary differential equations in time. The typical system size was $L_x=L_y=256$. Some test runs were made with $L_x=L_y=512$ and 1024. We used a uniform mesh size $\delta x=\delta y=1$ and time step $\delta t=2\times 10^{-2}$. The accuracy of calculations was checked by choosing $\delta x=\delta y=0.5$ and $\delta t=2\times 10^{-3}$. The dynamics of SD was computed over 6–7 decades in time, which allows monitoring the late stages of the phase separation process. Starting with random initial conditions with $|\psi|<0.01$, the characteristic length dynamics was calculated by averaging over 100 runs.

Without driving ($a=0$) one has the typical scenario of spinodal decomposition and there is no anisotropy in the behavior of l_x and l_y (Fig. 3). Thus initially the fastest mode grows in amplitude. At $t\sim 15$ (not shown) nonlinear saturation becomes important and sharp domain boundaries form. Then, at $t\sim 30$, the late stage coarsening starts where we observe the well-known scaling $l_x\sim l_y\sim t^{1/3}$. In Fig. 4 snapshots of the phase separation process are presented for a particular run.

We have found that in the 2D case, similar to one dimension, there exists a critical driving amplitude a_c above which the SD ends up in the stationary periodic solution with the period of the driving, i.e., striped structure. The critical amplitude turned out to be about $3\sim 5$ times larger than the one for one dimension. In particular, for $q=6\pi/L_x$ with $L_x=256$ one has in two dimensions $a_c=0.014$ whereas for one dimen-

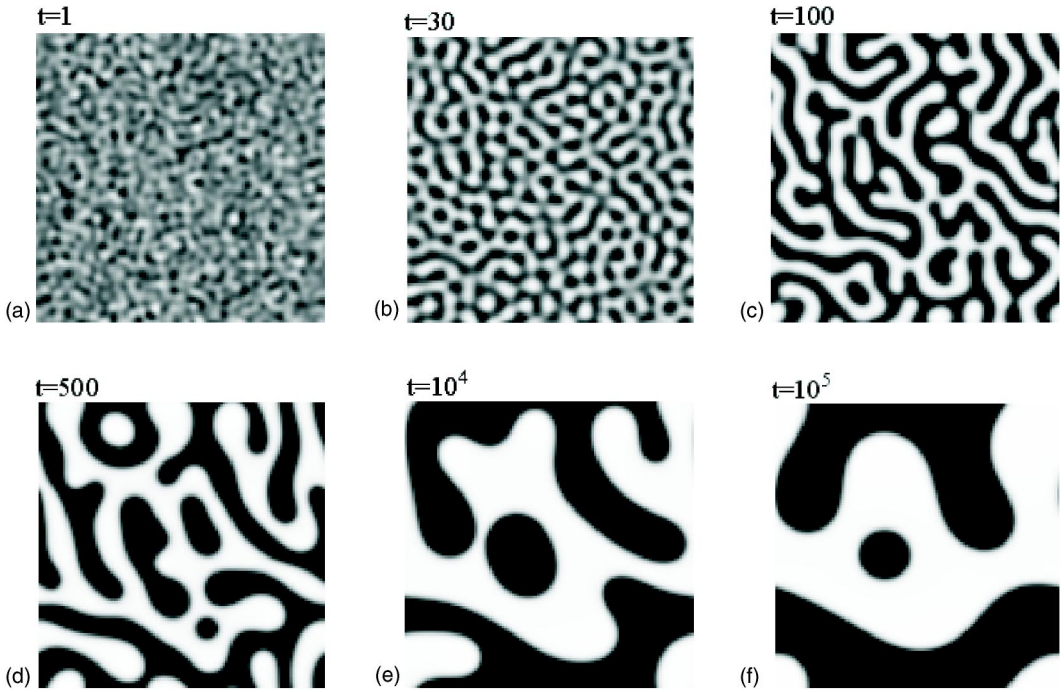

FIG. 4. Snapshots of the phase separation process. The same parameters as in Fig. 3.

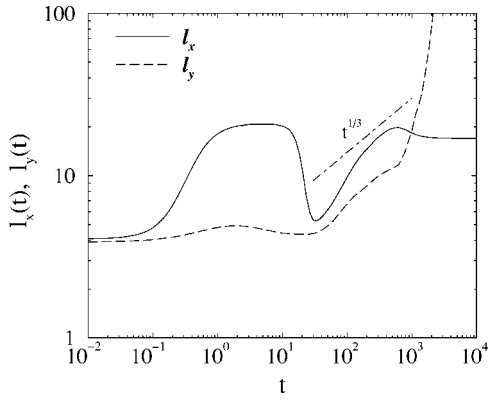

FIG. 5. Dynamics of the characteristic length scales $l_x(t)$ and $l_y(t)$ for the driving amplitude $a=0.05$ well above the critical. System size $L_x=L_y=256$, $\epsilon=1$, $q=6\pi/L_x$.

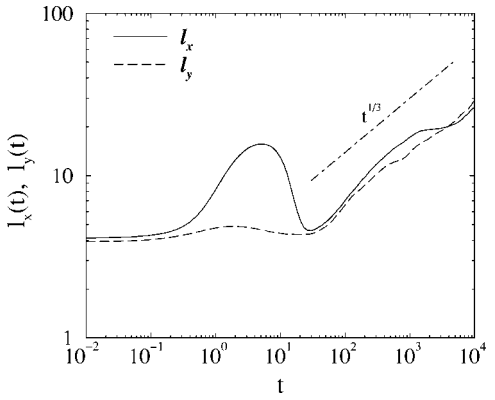

FIG. 7. Dynamics of the characteristic length scales $l_x(t)$ and $l_y(t)$ for the driving amplitude $a=0.01$ slightly below the critical. System size $L_x=L_y=256$, $\epsilon=1$, $q=6\pi/L_x$.

sion $a_c=0.0045$. Thus, for two dimensions the upper curve in Fig. 1 moves slightly upward (as will be argued below, the other curve remains unchanged).

In Fig. 5 the dynamics of the characteristic length scales l_x and l_y is presented for the case $a=0.05>a_c$ and in Fig. 6 typical snapshots are shown. The peculiar nonmonotonic behavior of l_x at early times can be understood as follows: in the linear range the noise-initiated fastest mode grows exponentially as $\psi_0 \exp(t/4)$ and the forced modulation with wave number q grows linearly as at (its exponential growth is small); see Eq. (17). Thus shortly after the quench the fastest mode determines the average domain size. At a time $t_1=(\psi_0/a)\exp(t_1/4)\sim\psi_0/a=0.2$ there is a crossover, beyond which the anisotropy becomes strong and l_x reaches a plateau that is controlled by the wave number of the forcing. Eventually, beyond $t_2=(\psi_0/a)\exp(t_2/4)\approx 18$, the exponential growth of the fastest mode wins, which leads to a drop of l_x. Although at this time nonlinearities are already noticable, the suppression of the effect of the forcing remains. Subsequently, one has essentially isotropic coarsening until l_x saturates at $1/q$. After this ($t>500$) the ordering in the y direction becomes exponentially fast. Actually the late stage remains essentially unchanged if the forcing is turned on as late as $t\sim 80$ where the average domain size has reached half the driving period. At a later time a forcing amplitude $a=O(1)$ is needed to generate the periodic state. In Figs. 7 and 8 we also show the dynamics of the characteristic length scales and snapshots for a driving amplitude slightly below the critical. One can see that at $t\sim 10^3$ there is competition between the influence of the forcing and the coarsening process, which finally wins.

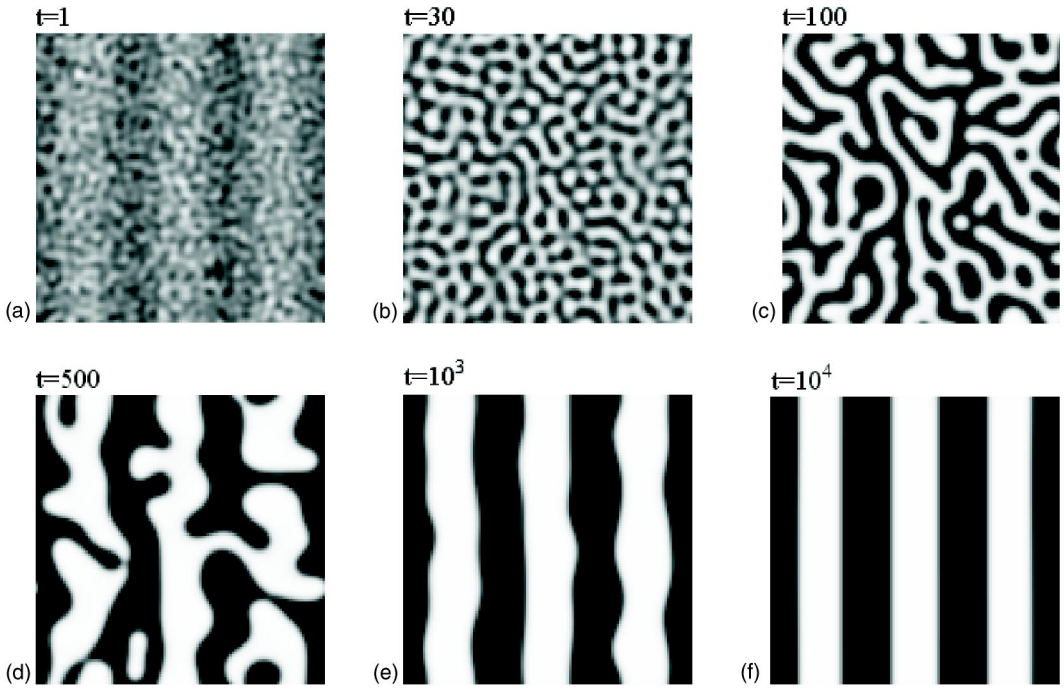

FIG. 6. Snapshots of the phase separation process. The same parameters as in Fig. 5.

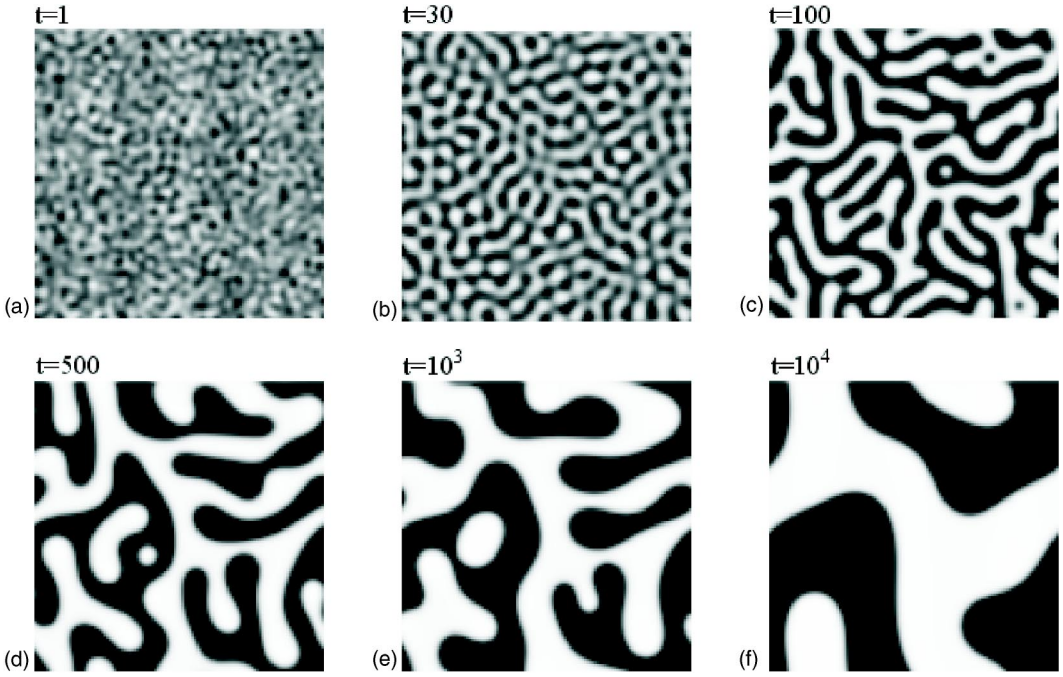

FIG. 8. Snapshots of the phase separation process. The same parameters as in Fig. 7.

V. DISCUSSION

We have determined analytically and numerically the forcing amplitude a_s necessary to stabilize in the Cahn-Hilliard equation a periodic stripe pattern against coarsening. a_s decreases rapidly with decreasing forcing wave number q. Interestingly, the destabilizing mode is of long-wave type, whereas the fastest-growing mode in the absence of forcing is of period-doubling type. This can be contrasted with phase separation in systems with nonconserved order parameter described by the Allen-Cahn equation, where both processes are controlled by long-wave modulations.

Although the result was established in one dimension, we expect it to hold also for a stripe pattern in two dimensions (i.e., a quasi-1D situation) because a stripe pattern is presumably not susceptible to transverse instabilities [17].

In addition we have determined by extensive simulations in one and two dimensions the critical forcing amplitude a_c necessary to produce a periodic stripe pattern from small random initial conditions. a_c depends only weakly on q. It essentially coincides with a_s for large q, of the order of the fastest growing linear mode. For small q, where the periodic pattern consists of an array of kinks, a_c is much larger than a_s. We have also done some numerical simulations with initial conditions appropriate to generate a periodic state by front propagation. In this way a critical amplitude only slightly smaller than a_c was found. We also noted that a small amount of (permanent) noise actually reduces a_c slightly.

The situation considered should be applicable to experiments on spinodal decomposition in sufficiently thin polymer films with small periodic temperature modulation created by means of optical grating technique. Then, for polymer blend layers of thickness less than a few micrometers the temperature variation across the film can be neglected for sufficiently small undercooling.

We now make connection with the polymer blends considered in Sec. II taking as an example the material parameters of polydimethylsiloxan (55%)/polyethylmethylsiloxan (45%) used in the experiments in Refs. [9,18]: $N_A=219.4$, $N_B=257.25$, $\alpha=2.9\times10^{-3}$, $\beta=3.22$ K, $T_c=313$ K, $\sigma_A=0.583$ nm, $\sigma_B=0.64$ nm (then $K=0.084$ nm^2), $D/|b|=(Mk_BT_c)/v=0.75\times10^{-6}$ cm^2/s, $D_T=2\times10^{-9}$ cm^2/(s K), and typical values for the temperature forcing amplitude $\delta T_0=0.2$ mK reachable in the optical grating experiments. One finds that for the temperature quench $T_c-T_0=2.5$ K (then $|b|=1.66\times10^{-4}$) the dimensionless driving amplitude in the experiments is about $a\approx10^{-2}$, which is of the order of the critical amplitude found in our simulations for two dimensions. For a quench of $T_c-T_0=2.5$ K, taking $v=4\pi(\sigma_A/2)^3/3$ and $V=4\pi r_m^3/3$ with $r_m=(K/|b|)^{1/2}$, one obtains for the dimensionless noise strength $g\approx10$. This is near the border of the Ginzburg criterion (19) $g\ll16\pi/3$.

It would be interesting to verify our finding that stabilization of a sufficiently long-wave periodic structure, once it has been established, can be achieved with extremely small amplitudes. Also, the prediction that the forcing may be applied with a time delay up to about 80τ after the quench may be tested experimentally. For the above parameters $\tau=0.04$ s, so a delay of 3 s should be allowed. Combining the two facts one concludes that the (relatively) high-amplitude forcing can probably be restricted to a rather short time interval. We plan to investigate the problem of optimal control of a prescribed pattern by determining the minimal light energy deposition required for its realization. This may involve also an optimization of the spatial profile of the forcing.

ACKNOWLEDGMENTS

This study was stimulated by experimental work by W. Enge and W. Köhler whom we thank for stimulating discus-

sions. Financial support by DFG through SFB481 "Komplexe Markomolekül- und Hybridsysteme in inneren und äußeren Feldern" is gratefully acknowledged.

APPENDIX

Here we derive the Ginzburg criterion in terms of the dimensionless noise strength g for Eq. (11) (in the absence of the forcing). In the two-phase region the Ginzburg criterion is $\langle[\delta\varphi(\mathbf{r},t)]^2\rangle \ll \varphi_{coex}^2$, where $\delta\varphi(\mathbf{r},t)$ gives the fluctuations of the order parameter and $\varphi_{coex}=\pm(|b|/u)^{1/2}$ is the mean-field value of the order parameter. The mean-square amplitude of the fluctuations can be calculated by averaging the Fourier back transform of the structure factor $S(\mathbf{k},t) \equiv \langle|\delta\varphi(\mathbf{k},t)|^2\rangle$ over a coarse-graining volume $V\sim r_m^d$,

$$\langle[\delta\varphi(\mathbf{r},t)]^2\rangle = \frac{1}{V}\int d\mathbf{r}\frac{1}{(2\pi)^d}\int d\mathbf{k}S(\mathbf{k},t)e^{i\mathbf{k}\cdot\mathbf{r}}. \quad \text{(A1)}$$

Note that $\langle\delta\varphi^2\rangle$ is necessarily sensitive to the consistent choice of the coarse-graining length r_m or, equivalently, to the upper cutoff in the integration over $\mathbf{k}$. From the linear evolution equation for the structure function

$$\frac{\partial S(\mathbf{k},t)}{\partial t} = 2\frac{Mk_BT_c}{v}(-k^2)[2|b| + Kk^2]S(\mathbf{k},t) + 2Mk_BT_ck^2 \quad \text{(A2)}$$

one finds

$$S(\mathbf{k},t)_{|t\to\infty} = \frac{v}{|b|(2+\xi^2k^2)}, \quad \text{(A3)}$$

and finally, under the assumption $r_m \gg \xi$, for the mean-square amplitude of the fluctuations

$$\langle[\delta\varphi(\mathbf{r},t)]^2\rangle = \frac{v}{2V}|b|^{-1}. \quad \text{(A4)}$$

Actually, for the purpose of estimates this expression can be taken down to $r_m \approx \xi$. Then the Ginzburg criterion in terms of the dimensionless noise strength g gives

$$g \ll 4V(K/|b|)^{-d/2}. \quad \text{(A5)}$$

[1] J. D. Gunton, M. San Miguel, and P. S. Sahni, in *Phase Transitions and Critical Phenomena*, edited by C. Domb and J. L. Lebowitz (Academic, London, 1983), Vol. 8.

[2] A. J. Bray, Adv. Phys. **43**, 357 (1994).

[3] T. Hashimoto, K. Matsuzaka, E. Moses, and A. Onuki, Phys. Rev. Lett. **74**, 126 (1996).

[4] A. M. Lacasta, A. Hernandez-Machado, and J. M. Sancho, Phys. Rev. B **48**, 9418 (1993).

[5] Y. Jayalakshmi, B. Khalil, and D. Beysens, Phys. Rev. Lett. **69**, 3088 (1992).

[6] H. Tanaka and T. Sigehuzi, Phys. Rev. Lett. **75**, 874 (1995); J. Okinaka and Q. Trang-Cong, Physica D **30**, 84 (1995).

[7] Q. Trang-Cong, in *Structure and Properties of Multiphase Polymeric Materials*, edited by T. Araki, Q. Trang-Cong, and M. Shibayama (Marcel Dekker, New York, 1998).

[8] S. Wiegand and W. Köhler, in *Thermal Nonequilibrium Phenomena in Fluid Mixtures*, edited by W. Köhler and S. Wiegand (Springer, Heidelberg, 2002), p. 189.

[9] W. Enge and W. Köhler, Phys. Chem. Chem. Phys. **6**, 2373 (2004).

[10] S. R. de Groot and P. Mazur, *Non-Equilibrium Thermodynamics* (North-Holland, Amsterdam, 1962).

[11] J. W. Cahn and J. E. Hilliard, J. Chem. Phys. **28**, 258 (1958); H. E. Cook, Acta Metall. **18**, 297 (1970).

[12] F. S. Bates, G. D. Wignall, and W. C. Koehler, Phys. Rev. Lett. **55**, 2425 (1985).

[13] P. C. Hohenberg and B. I. Halperin, Rev. Mod. Phys. **49**, 435 (1977).

[14] K. Binder, J. Chem. Phys. **79**, 6387 (1983).

[15] S. C. Glotzer, Annu. Rev. Comput. Phys. **2**, 1 (1995).

[16] J. S. Langer, Ann. Phys. (N.Y.) **65**, 53 (1971).

[17] D. Bettinson and G. Rowlands, Phys. Rev. E **54**, 6102 (1996).

[18] G. Meier, B. Momper, and E. W. Fischer, J. Chem. Phys. **97**, 5884 (1992).